IBRACON Structures and Materials Journal
Revista IBRACON de Estruturas e Materiais
ISSN 1983-4195 ismj.org

ORIGINAL ARTICLE

Exploring the behavior and quality control of steel fiber reinforced concrete through 3-point bending test and Montevideo test

Investigando o comportamento e o controle de qualidade do concreto reforçado com fibras de aço baseado no ensaio de flexão em três pontos e no ensaio Montevidéu

Gabriela Mazureki Campos Bahniuk[a,b]
Ricardo Pieralisi[a]
Roberto Dalledone Machado[a]

[a]Universidade Federal do Paraná – UFPR, Centro de Estudos de Engenharia Civil – CESEC, Programa de Pós-graduação em Engenharia Civil – PPGEC, Curitiba, PR, Brasil
[b]Universidade Estadual de Ponta Grossa – UEPG, Ponta Grossa, PR, Brasil

Received 14 November 2023
Revised 12 March 2024
Accepted 05 May 2024

Abstract: Residual tensile strength plays a critical role in the design of steel fiber-reinforced concrete (SFRC) elements. It is imperative to verify and control the mechanical properties through experimental tests. This study investigates an alternative test method, known as the Montevideo (MVD) test, by assessing SFRC properties with different fiber contents (0.5%, 0.75%, and 1.0%). The experimental program included three key aspects: i) determination of residual tensile loads and strength through the three-point bending (3PBT) test presented by NBR 16940/EN 14651; ii) determination of the residual tensile loads through the MVD test, correlatable with 3PBT results; iii) assessment of concrete in different ages: 28 days and 100 days. The results reveal a correlation factor (k_{MVD}) that translates MVD test loads into values specified by NBR 16940/EN 14651, with a dependence on fiber content.

Keywords: steel fiber reinforced concrete, residual tensile strength, Montevideo test, quality control.

Resumo: A resistência à tração residual desempenha um papel crítico no projeto de elementos de concreto reforçado com fibra de aço (CRFA). É imperativo verificar e controlar as propriedades mecânicas por meio de ensaios experimentais. Este estudo investiga um método de teste alternativo, conhecido como Montevidéu (MVD), para avaliar as propriedades do CRFA, com diferentes volumes de fibra (0,5%, 0,75% e 1,0%). O programa experimental incluiu três aspectos principais: i) determinação das cargas residuais de tração e resistência pelo ensaio de flexão em três pontos (3PBT) apresentado pela NBR 16940/EN 14651; ii) determinação das cargas de tração residuais pelo ensaio MVD, correlacionáveis com os resultados do 3PBT; iii) avaliação do concreto nas diferentes idades: 28 dias e 100 dias. Os resultados revelam um fator de correlação (k_{MVD}) que transforma as cargas de ensaio MVD naquelas especificados pela NBR 16940/EN 14651, com dependência do teor de fibra.

Palavras-chave: concreto reforçado com fibras de aço, resistência à tração residual, teste Montevideu, controle de qualidade.

How to cite: G. M. C. Bahniuk, R. Pieralisi, and R. D. Machado, "Exploring the behavior and quality control of steel fiber reinforced concrete through 3-point bending test and Montevideo test," *Rev. IBRACON Estrut. Mater.*, vol. 17, no. 4, e17414, 2024, https://doi.org/10.1590/S1983-41952024000400014

Corresponding author: Gabriela Mazureki Campos Bahniuk. E-mail: gabriela.campos@uepg.br
Financial support: Project CNPq/MCTI/FNDCT Nº 18/2021 422189/2021-9; CNPq - grant number: 316985/2021-0, and the institutional project CAPES-PRINT/UFPR.
Conflict of interest: Nothing to declare.
Data Availability: The data that support the findings of this study are available from the corresponding author GMCB, upon reasonable request.

1 INTRODUCTION

Steel Fiber-Reinforced Concrete (SFRC) is a composite material that exhibits an enhancement in residual tensile strength due to the incorporation of dispersed fibers. The addition of fibers enhances the overall performance of SFRC elements and modifies their behavior after cracking, providing improved residual strength (commonly referred to as toughness) and ductility [1]–[6]. When fibers are present, they modify the mechanism of crack formation and propagation by facilitating the transfer of tensile forces across the cracks via the fibers. This leads to tension in the concrete due to both bond stress and fiber bridging [7].

According to Di Prisco et al. [4], as fiber reinforcement mechanisms are mainly activated after the concrete matrix cracking, fibers have little influence on the behavior of uncracked elements. Thus, residual tensile strength (post-cracking), which represents an important design parameter for SFRC structures, is the mechanical property most influenced by the inclusion of fibers, as concluded by Larsen and Thorstensen [6]. Therefore, to increase the utilization of SFRC in structural applications, it is important to accurately establish the residual tensile strength of SFRC.

Several standards and guidelines present constitutive laws for the design of SFRC [8]–[12], and their use is directly related to post-cracking tensile behavior [13]. To determine the mechanical properties, indirect tensile tests are commonly used, such as the three-point bending (3PBT) test presented by NBR 16940 [11] and EN 14651 [12]. This test is recommended to parameterize the residual strength for corresponding crack openings and thus obtain the constitutive law to be applied in the structural design of SFRC elements.

The three-point test is performed on a prismatic specimen with a cross-sectional area of 150×150 mm, a total length between 550 mm and 700 mm, as a single-supported beam with a span of 500 mm. From the test, a force vs. displacement curve expressed in CMOD (Crack Mouth Opening Displacement) is plotted, corresponding to the crack opening on the bottom. Some characteristics of the 3PBT test execution include the size and weight of specimens, the time consumption, the requirement of specific test equipment, and the difficulty in extracting specimens if necessary.

Thus, other types of compact tests (smaller specimens) can be performed to determine the residual tensile strength of concrete, such as the Double Punch test, proposed by NBR 16939 [14], the Wedge-Splitting test (WST), method as described in Brühwiler and Wittmann [15]; the Barcelona test (BCN), proposed by Molins et al. [16]; the Double Edge Wedge Splitting test (DEWS), test proposed by Di Prisco et al. [17], and the Montevideo test (MVD) proposed by Segura-Castillo et al. [18]. These tests can be correlated with the 3PBT test for quality control.

The MVD test predominantly derives from the WST test, but adjustments have been implemented to simplify preparation and testing procedures [18]. The test was proposed for SFRC with softening behavior and can be performed on casted or extracted specimens. A 150 mm cubic specimen with a notched cut measuring 25 mm in depth and 5 mm in width is suggested for the test. This specific specimen and notch geometry were chosen to replicate the fracture surface of the EN 14651 test [12], thereby preventing any scale effects in the correlation of their outcomes. The specimen is simply-supported on the base, and the loading device is a solid wedge inclined. Each side of the wedge has a 15º slope concerning the vertical direction; therefore, the total wedge angle is 30º. For theoretical analysis, it is assumed that only one crack is formed after cracking, which starts at the tip of the notch and extends towards the support, dividing the specimen into two halves that rotate as rigid bodies relative to the support point. After the test, it is possible to determine the displacements at the notch tips. Furthermore, a linear relationship between wedge displacement and CMOD was observed in Segura-Castillo et al. [18]. Therefore, it is possible to carry out the test relying only on the stroke displacement, thus avoiding the placement of external displacement transducers and simplifying the test.

However, the authors emphasize the necessity for further research, considering that the Montevideo test is rarely utilized and lacks standardization. Therefore, additional applications are important to enhancing understanding of the method and its outcomes, including the correlation factor between loads concerning the 3PBT test for different mix designs and fiber contents. In this context, this study aims to explore the MVD test as a simplified approach for quality control in FRC.

2 METHODOLOGY

2.1 Material properties, compositions and specimens

The SFRC mixture (Figure 1) consisted of: Brazilian cement CPV-ARI, referred to as Type III by ASTM C150/C150M (Figure 1a), with a density of 3120 kg/m^3, and limestone filler (Figure 1b) showing a density of 2800 kg/m^3 that served as the binder in all the mixtures. Natural sand (Figure 1c), showing a density of 2630 kg/m^3, unit weight of 1.53 g/cm^3, water absorption of 0.72%, and a fineness modulus of 1.87, along with diabase aggregate (Figure 1d), having a density of 2990 kg/m^3, unit weight of 1.56 g/cm^3, water absorption of 0.94%, and a maximum particle size of 12.5 mm, were used as the fine and coarse aggregate, respectively. To ensure appropriate workability, a polycarboxylate superplasticizer (specifically MC-PowerFlow 1180 with a specific weight of 1.09 g/cm^3) was added. Additionally, short-end-hooked steel

fibers (DRAMIX 3D 65/35 BG - Figure 1e), with a length of 35 mm, diameter of 0.55 mm, aspect ratio of 65, and tensile strength of 1345 MPa, were employed as reinforcement.

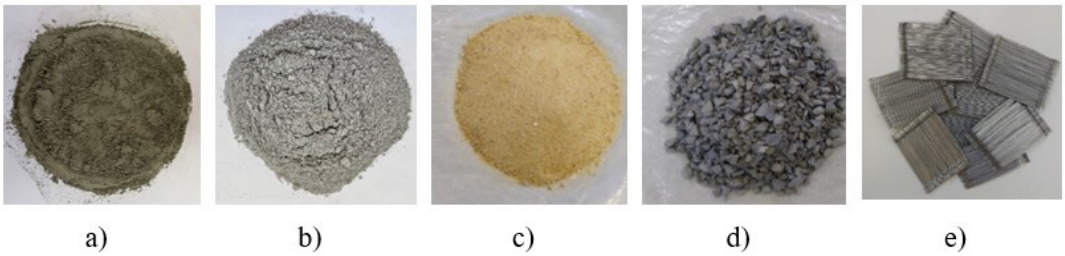

Figure 1. SFRC ingredients: a) cement; b) limestone filler; c) natural sand; d) coarse aggregate; e) steel fibers.

Table 1 presents the concrete mixtures used in this study. Adjustments to the coarse aggregate content were required to accommodate the increase in steel fiber volume. Also, the quantity of superplasticizer required for each mixture varied to ensure equivalent fresh properties of the SFRC. The nomenclature for the several concretes made was SFRC (steel fiber-reinforced concrete), followed by the indication of the volume fractions of steel fibers (V_f) adopted, that is, SFRC0.50, SFRC0.75, and SFRC1.00.

Given that the consolidation method has a known impact on the distribution and orientation of steel fibers and, subsequently, on the performance of SFRC [19], the specimens were consolidated exclusively using external vibration via rubber hammer blows, particularly because the concrete had a more fluid consistency.

Table 1. SFRC mixtures composition.

Concrete	Concrete mix design (kg/m³)						V_f (%)	Superplasticizer (%)
	Cement	Limestone filler	Water	Sand	Coarse aggregate	Steel fiber		
SFRC0.50	436	70	183.1	872	946.1	39.25	0.50	1.4
SFRC0.75	436	70	183.1	872	937.4	58.88	0.75	1.6
SFRC1.00	436	70	183.1	872	928.7	78.50	1.00	1.7

In total, fourteen cylindrical specimens of size 100x200 mm were cast for each mixture composition, ten for compressive strength and four for modulus of elasticity. Compressive strength characterization tests were conducted at 28 days on four specimens and 100 days on six specimens. The specimens were also tested approximately three months after concreting, considering that initial high-strength cement was used and that small differences in this test age would not be significant. The modulus of elasticity specimens was tested only at 28 days.

Six prismatic specimens measuring 150x150x550 mm for each mixture composition were tested at 28 days for flexural tensile strength (3PBT). A notch 25 mm deep and 5 mm thick was made in the middle of the specimen span, as illustrated in Figure 2.

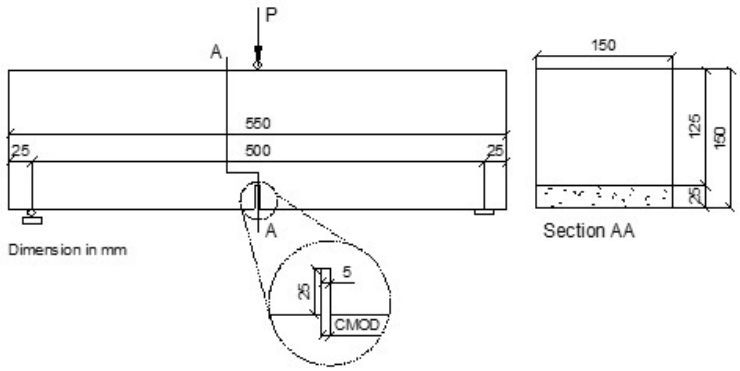

Figure 2. Specimen for three-point flexural beam test.

Nine cubic specimens of 150x150x150 mm for each mixture composition were tested by MVD, and the test was conducted on four specimens at 28 days and on five specimens at 100 days. To optimize the number of specimens, in addition to the cubic specimens (Figure 3a), half of each prismatic beam specimen was also tested after the flexural tensile strength tests, as indicated in Figure 3b. Each beam resulted in two parts; one part was tested at 28 days, and the other was tested at 100 days. All the MVD specimens were notched following the same dimension and orientation as the flexural beam. In the prismatic specimens, the notches were made at the midpoint between the load application point and the support of the 3PBT. It is emphasized that the asymmetry does not affect the results, as the bending moment generated due to this difference is negligible, and any resulting rotation can be disregarded. Steel angles were affixed to minimize friction between the loading wedge and the specimen, and a multi-function lubricant (WD-40) was applied to the contact surface. Inductance tests were previously carried out with the nine cubic specimens. Figure 4 presents a flowchart with a summary of the tests.

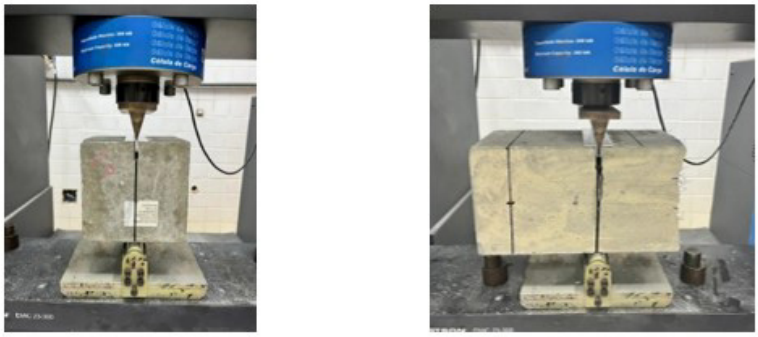

a) b)

Figure 3. MVD test: a) Cubic specimen; b) Half of the beam.

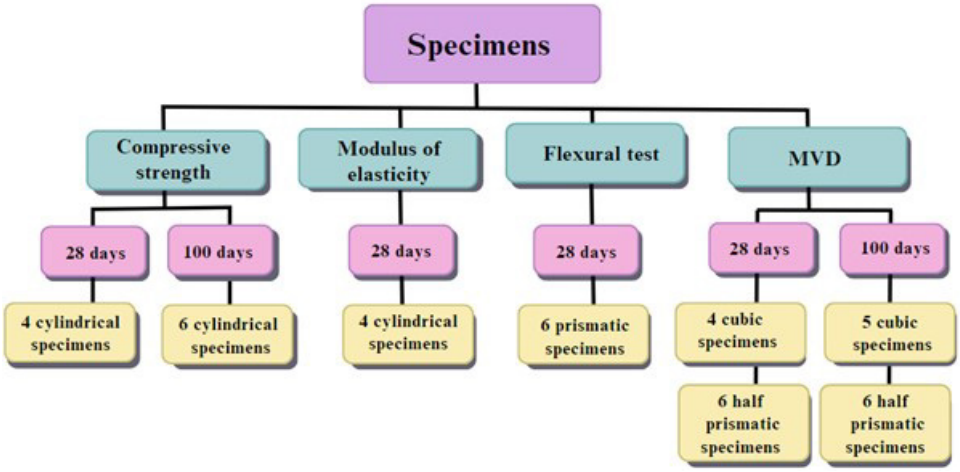

Figure 4. Summary of the tests.

The cylindrical and cubic specimens were cast from the same concrete casting (tilting drum mixer with four hundred liters of nominal capacity), while the prismatic specimens were made the following day in another concrete casting (tilting drum mixer with one hundred and twenty liters of nominal capacity). Furthermore, considering the capacity of the concrete mixer and the volume of concrete required for casting, two batching operations were carried out for both the cylindrical/cubic specimens and the prismatic specimens. The average values were presented in this study.

For the curing of the cylindrical and cubic specimens, a glass surface was positioned on top of the molds for the initial 48 hours. Subsequently, the specimens were demolded and submerged in water until reaching 28 days. As for the prismatic specimens, demolding also occurred after 48 hours of casting. After 24 hours, the top of the specimen was wetted and covered with a wet drainage mat and plastic sheeting. From that point until 28 days, the prismatic specimens were wetted daily.

2.2 Tests procedures

2.2.1 Characterization in terms of slump, compressive strength and modulus of elasticity

The SFRC control in the fresh state was carried out according to the slump test and considering that the concrete has characteristics of self-compacting concrete, the slump flow was also determined by the Abrams cone method according to recommendations of NBR 15823-1 [20] and NBR15823-2 [21].

The compressive strength was evaluated according to methods NBR 5739 [22] and C39/C39M-18 [23], and the modulus of elasticity according to methods NBR 8522-1 [24] and C469/C469M-14 [25].

2.2.2 Flexural tensile strength test NBR 16940 [11] and EN 14651 [12]

Prismatic specimens were tested by NBR 16940 [11] and EN 14651 [12] for each mixture composition. An Instron machine model EMIC 23-300, operating under deflection control, was employed to generate comprehensive CMOD-load curves (see Figure 5).

The CMOD was estimated using Equation 1 proposed by NBR 16940 [11]:

$$\delta = 0.85CMOD + 0.04 \quad (1)$$

Where δ represents the deflection, in mm; CMOD denotes the Crack Mouth Opening Displacement, in mm.

Figure 5. Flexural beam test.

The flexural strengths were obtained according to Equation 2, where $f_{R,j}$ represents the residual strengths; F_j is the load measured corresponding to the crack openings in 0.5 mm, 1.5 mm, 2.5 mm, and 3.5 mm, *l* refers to the span; b is the width of the specimen; h_{sp} is the distance between the tip of the notch and the top of the specimen in the mid-span section.

$$f_{R,j} = \frac{3.F_j.l}{2.b.h_{Sp}^2} \quad (2)$$

To identify and handle any outlier results, statistical treatment using the Grubbs test, as proposed by NBR 16938 [26], was applied to investigate the obtained results.

After the flexural tensile strength test, the specimens were divided at the fracture plan into two parts, denominated part 1 and part 2. The fiber count was performed on each side considering nine quadrants, allowing for the determination of the total fiber quantity as well as the fiber distribution (Figure 6).

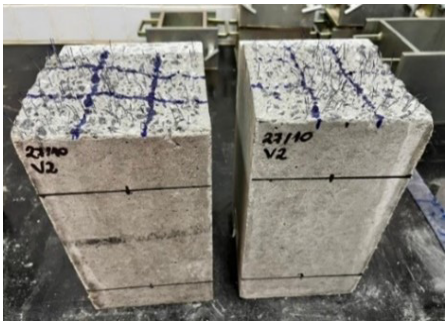

Figure 6. Delimitation quadrants for counting fibers in the prismatic specimens.

2.2.3 MVD test

The MVD test was conducted following the methodology proposed by Segura-Castillo et al. [18] with the same equipment used for the flexural beam test. CMOD was determined according to Equation 4 and illustrated in Figure 7.

$$tan\theta = \frac{w_M}{h} \tag{3}$$

$$w_M = 2.\delta.tan\alpha \tag{4}$$

Where h is the height of the specimen; θ is the relative rotation between the two halves of the specimen; δ is the displacement of the testing machine; w_M denotes the CMOD, and α is the angle of the solid wedge (30º).

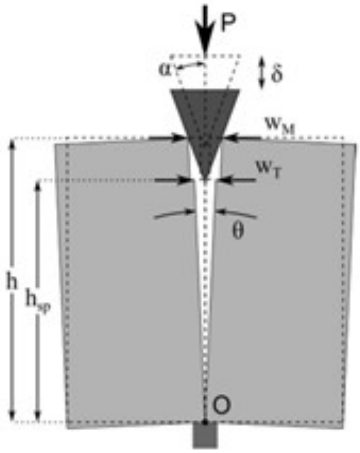

Figure 7. Behavior of the MVD specimen after the beginning of the cracking.

2.2.4 Inductive test

The inductive test [27]–[29] was employed to estimate the steel fiber content and orientation in all cubic specimens. The inductive test is a non-destructive technique based on Faraday's first law of electromagnetic induction. Assessing changes in the electromagnetic field within the apparatus before and after the test can quantitatively estimate the content and orientation of steel fibers [27], [28]. The equipment used (see Figure 8a) includes an LCR meter and two winding coils connected in series that received an electric current, generating a magnetic field [30]. The steel fiber inside the specimens, when placed inside the apparatus (Figure 8b), alters the magnetic field and induces a change in inductance, which can be measured by the LCR meter.

To estimate the steel fiber content (C_f) and orientation (C_i, where i is related to the three orthogonal axes x, y, and z – see Figure 8c), the change in inductance (L_i) for each orthogonal axis is measured. This is achieved by positioning the cubic specimen with each axis orientated longitudinally to the winding coils. Three measurements were recorded for each axis. The C_f was estimated using Equations 5, where ω represents the proportionality constant equal to 1.8796 kg/(m^3.mH) for the equipment used, and L_e is the sum of the changes in inductance measurements for the three axes. The C_i was determined for each axis using Equation 6, where α_i is the orientation number, calculated with Equation 7 where γ is a constant that depends on the type of fiber and the coil configuration, equal to 0.058 for the analyzed fiber.

$$C_f = \omega.L_e \tag{5}$$

$$C_i = \frac{\alpha_i}{\sum_{i=x.y.z}\alpha_i} \tag{6}$$

$$\alpha_i = 1.03.\sqrt{\frac{L_i.(1+2.\gamma)-L_e.\gamma}{L_e.(1-\gamma)}} - 0.1 \tag{7}$$

Figure 8. Inductive test: a) equipment; b) specimen; c) concreting face identification (CF).

3 RESULTS AND ANALYSES

3.1 Fresh state properties

Regarding the properties of the concrete in the fresh state, Table 2 demonstrates the slump and the spread of concrete. According to NBR 8953 [32], all concrete mixes achieved the highest slump class, i.e., slump ≥ 220 mm. However, the slump test is typically applicable to concretes within the slump class range of S10 to S220 [31]. It is observed that for SFRC0.50 and SFRC0.75 mixes, the slump values exceeded the established limit.

Table 2. Properties of concrete in the fresh state: slump, slump-flow, and viscosity.

Concrete	Specimens	Slump (mm)	Slump-flow (mm)	t_{500} (s)
SFRC0.50	cylindrical/cubic	265*	693	14
	prismatic	258*	618	14
SFRC0.75	cylindrical/cubic	235*	660	12
	prismatic	235*	590	19
SFRC1.00	cylindrical/cubic	223	581	17
	prismatic	220	495	-

t_{500}: time interval, in seconds, between the start and end of concrete pouring, from the mold diameter (200 mm) to the circular mark of diameter 500 mm on the base plate. * slump values that exceeded the normative limit [31]

Regarding slump flow results, according to NBR 15823-1 [20], the spread class for most mixes was SF1 (550 to 650 mm), except for SFRC0.50 and SFRC0.75 – cylindrical/cubic specimens, which were classified as SF2 (660 to 750 mm), and SFRC1.00 – prismatic specimens, which had a spread below the minimum value of 550 mm and did not reach the diameter of 500 mm. As for the apparent viscosity class (t_{500}), all concretes were classified as VS2, as they have a time greater than 2 seconds. The SFRC0.75 prismatic specimens result in higher t_{500} values.

Figure 9 demonstrates the spread of concrete. Through visual observation, the concretes exhibited slight bleeding, especially SFRC1.00, but no segregation occurred in any mix. All mixes maintained good workability, including concrete with a fiber volume of 1.0%.

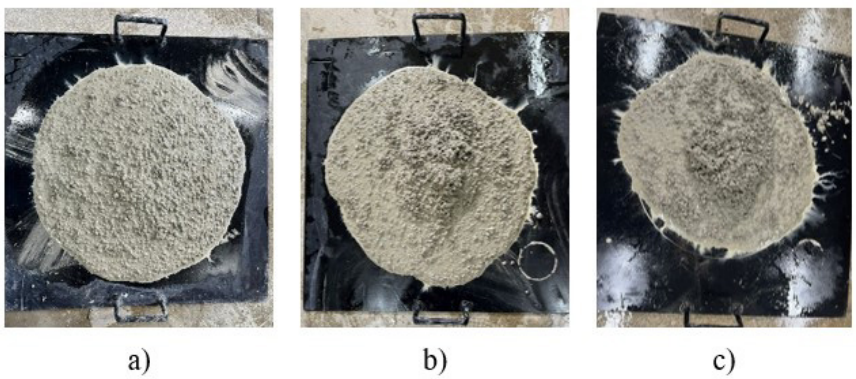

Figure 9. Slump-flow of concretes: a) SFRC0.50; b) SFRC0.75; c) SFRC1.00

3.2 Compressive strength and modulus of elasticity

Table 3 presents the compressive strength and modulus of elasticity for all compositions, with the standard deviation (SD) and coefficient of variation (CV). To assess the impact of fiber volume on compressive strength and modulus of elasticity and evaluate the strength increase over time, an analysis of variance (ANOVA) was performed using Tukey's method for comparison, with a significance level of 5%.

Table 3. Compressive strength of concretes.

Concrete	f_c (MPa)							E_c (GPa)		
	$f_{c,28}$	SD	CV (%)	$f_{c,100}$	SD	CV (%)	$f_{c,100}/f_{c,28}$ (%)	$E_{c,28}$	SD	CV (%)
SFRC0.50	58.39	2.25	3.92	75.66	2.62	3.46	29.6	46.80	1.82	3.90
SFRC0.75	51.22	4.79	9.35	70.17	7.06	10.06	37.0	47.18	3.17	6.72
SFRC1.00	59.75	0.91	1.52	71.59	3.57	4.99	19.8	52.86	0.72	1.36

fc,28: Compressive strength at 28 days; fc,100: Compressive strength at 100 days; Ec,28: modulus of elasticity at 28 days

The average compressive strength for all compositions ranged from 51 MPa to 60 MPa at 28 days and from 70 MPa to 75 MPa at 100 days. Evaluating the influence of steel fiber inclusion on compressive strength, it can be seen that, at 28 days, there was a significant difference in the strengths of the SFRC0.50, SFRC0.75, and SFRC1.00 concretes, with the SFRC0.75 concrete showing significantly different values. However, at 100 days, the analysis of variance indicated that there were no significant differences in the strengths of the SFRC0.50, SFRC0.75, and SFRC1.00 concretes (p-value of 0.157). It was observed that the difference in strength exhibited by SFRC0.75 concrete at 28 days was 'compensated' over time, and the inclusion of fibers did not result in an increase in compressive strength. Furthermore, the SFRC0.75 concrete showed the highest standard deviations for both ages, followed by the SFRC0.50 concrete.

The greatest increase in strength during this period was seen in the SFRC0.75 concrete, in the order of 37 percent in the average strength of the concrete, while the smallest increase was 19.8 percent for the SFRC1.00 concrete. For the same mix, the compressive strengths at 28 days and 100 days were significantly different, showing an increase in compressive strength during this period, even with the use of CPV-ARI cement with a high initial strength.

The Tukey test indicated that there was a statistically significant difference (p-value of 0.005) in the modulus of elasticity between SFRC1.00 and the other two compositions, SFRC0.50 and SFRC0.75. This suggests that the presence of a higher volume fraction of steel fibers (1.0%) influenced the modulus of elasticity, leading to a different response compared to the mixtures with lower fiber volumes.

In the literature, some researchers report that the addition of fibers does not affect the modulus of elasticity and compressive strength of concrete [33]–[36], others observe a reduction in the modulus of elasticity with an increase in compressive strength [37], and some note an increase in the modulus of elasticity with an increase in fiber content [38], as occurred in this study. Other investigations found an increase in compressive strength as a result of the inclusion of fibers [39]–[42]. Nonetheless, increasing the fiber content may have a detrimental effect on the compressive strength of very high fiber volumes [43], [44], as an excessive amount of fibers can also lead to increased voids and microcracks in the concrete matrix, thereby rendering the concrete more brittle [44].

3.3 Residual tensile strength from three-point bending test

Figure 10 shows the Load vs. CMOD curves of all the prismatic specimens and the average curves highlighted in bold lines. All curves exhibit strain-softening behavior, and residual strength increases with the fiber content.

Table 4 presents the average values of flexural strength (f_{PEAK}) and residual strengths (f_{R1}, f_{R2}, f_{R3}, and f_{R4}), which were determined at CMOD values of 0.5, 1.5, 2.5, and 3.5, respectively. Additionally, the table includes standard deviation (SD) and the coefficient of variation (CV) for these parameters.

All the compositions presented CV exhibited 25%, which is a limit specified in NBR 16938 [26]. SFRC0.75 exhibited the highest coefficient of variation, while SFRC 0.50 exhibited the lowest coefficient of variation.

Analyzing the average values with the Tukey test, it was observed that for all variables (f_{PEAK}, f_{R1}, f_{R2}, f_{R3}, and f_{R4}) there was a statistically significant difference only between SFRC0.50 and the other two compositions regarding flexural strength and residual strengths. It is known that the magnitude of the residual strength of SFRC depends on the properties of the concrete matrix (it is found that there was no significant difference in compressive strength between the concretes), the steel fibers applied (the same type was adopted for all compositions) and the fiber content. Generally, residual strength increased with the fiber content, aligning with the literature [1]–[3], [7], [45]–[47]. However, despite this increase, the load values from a CMOD of 1.5 mm were quite similar between SFRC0.75 and SFRC1.00

compositions. This suggests that beyond a certain threshold, increasing the volume of fibers may not guarantee a corresponding increase in the residual strength of the specimen.

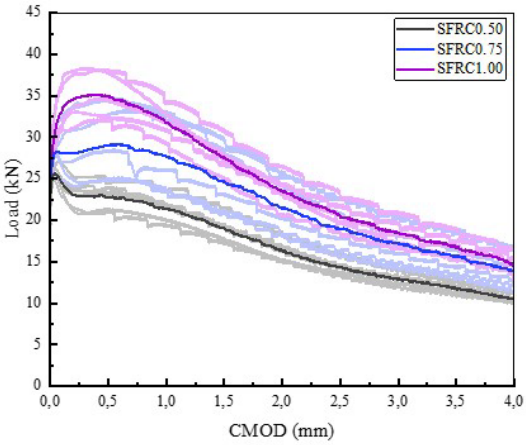

Figure 10. Load vs. CMOD of all concretes.

Table 4. Residual strength at crack openings of 0.5, 1.5, 2.5 e 3.5 mm ($f_{R,1}$, $f_{R,2}$, $f_{R,3}$, $f_{R,4}$) for flexural beam test.

Concrete		f_{PEAK} (MPa)	$f_{R,1}$ (MPa)	$f_{R,2}$ (MPa)	$f_{R,3}$ (MPa)	$f_{R,4}$ (MPa)
SFRC0.50	Mean	7.57	6.68	5.58	4.18	3.40
	SD	0.18	0.40	0.42	0.25	0.17
	CV (%)	2.45	6.07	7.52	5.86	4.94
SFRC0.75	Mean	9.00	8.75	7.35	5.60	4.60
	SD	1.11	1.33	1.80	0.93	0.76
	CV (%)	12.39	15.25	16.12	16.60	16.55
SFRC1.00	Mean	10.10	9.96	7.81	5.47	4.73
	SD	0.70	0.73	0.65	0.56	0.53
	CV (%)	7.02	7.32	8.26	9.70	11.04

Complementing the analysis, Figure 11 illustrates the number of fibers found in the fracture section of the prismatic specimens following the 3PBT. Among the specimens with the same fiber volume, the coefficient of variation for the total number of fibers was: 5% for SFRC0.50, with a mean of 275 fibers and a standard deviation of 14 fibers; 15.28% for SFRC0.75, with a mean of 383 fibers and a standard deviation of 58 fibers; and 11.05% for SFRC1.00, with a mean of 444 fibers and a standard deviation of 49 fibers. SFRC0.75 exhibited the highest coefficient of variation in the number of fibers, which aligns with the observed mechanical behavior.

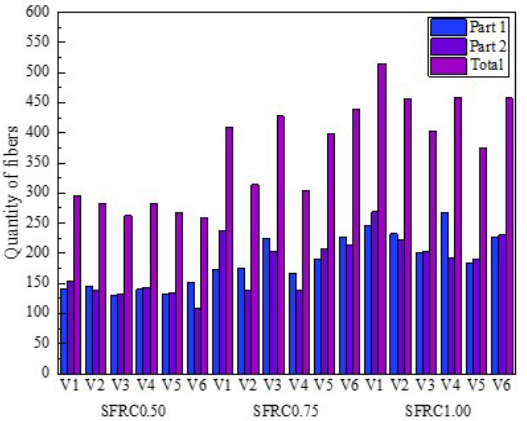

Figure 11. Quantity of fibers vs. fiber content.

Another characteristic was that, as expected, the total fiber quantity increased between SFRC0.50, SFRC0.75, and SFRC1.00 concretes. According to the variance analysis, the fiber quantity for SFRC0.50 showed a significant difference compared to the others, while the same was not observed between SFRC0.75 and SFRC1.00. It was worth noting that, in the analysis of residual strengths, a significant difference had already been observed only for concrete SFRC0.50.

Regarding the fiber distribution in the cross-section of the prismatic specimen (Figure 12), it can be observed that, for the SFRC0.50 mix, a higher quantity of fibers is concentrated on the bottom face of the beam. However, for SFRC0.75 and SFRC1.00, this characteristic is not predominant, suggesting a more homogeneous internal distribution of steel fibers. Additionally, in the majority of specimens, the quantity of fibers in the section (after separation) is similar on both sides.

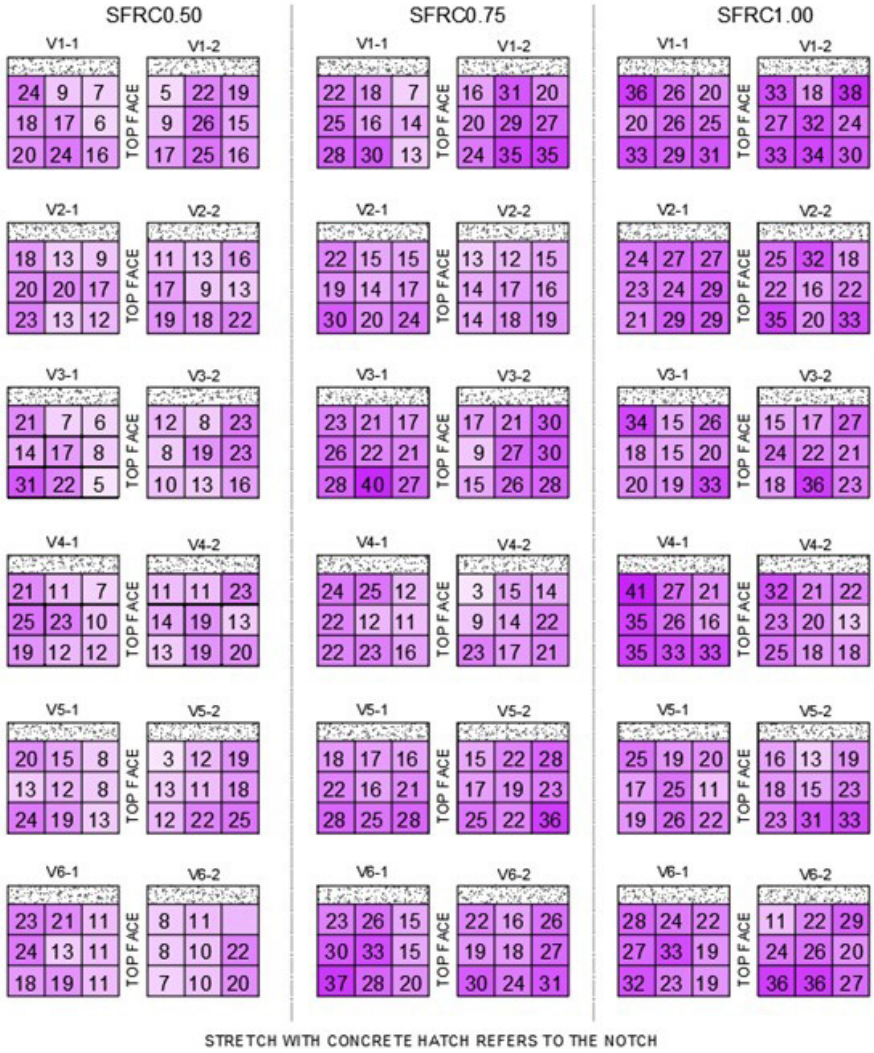

Figure 12. Fiber distribution in the prismatic specimens.

3.4 Effective fiber content - Inductive test

Inductive tests were conducted on the cubic specimens, allowing the determination of incremental inductance values along the three axes. Subsequently, the fiber content (C_f) of each cubic specimen was calculated using Equation 5. The percentages of inductance along the three axes were calculated using Equations 6 and 7. Table 5 presents the results of the average fiber content ($\overline{C_f}$) and the average fiber orientation, in percentage, in each axis ($\overline{C_x}$, $\overline{C_y}$, and $\overline{C_z}$) determined through the inductive test. Additionally, the table includes the standard deviation (SD) and the coefficient of variation (CV) for these parameters. An incident occurred during the mixing of one SFRC0.50 batch, where the concrete mixer malfunctioned, leading to an uneven distribution of fibers. Consequently, the data from the cubic specimens (SFRC0.50-batch 1) were excluded from the analysis.

Table 5. Fiber distribution results based on inductive test.

Concrete	$\overline{C_f}$ (kg/m³)			$\overline{C_x}$ (%)			$\overline{C_y}$ (%)			$\overline{C_z}$ (%)		
	Mean	SD	CV (%)	Mean	SD	CV (%)	Mean	SD	CV (%)	Mean	SD	CV (%)
SFRC0.50	46.19	3.13	6.78	36.43	1.64	4.49	36.69	1.55	4.22	26.88	2.08	7.73
SFRC0.75	63.76	4.89	7.67	37.16	1.59	4.27	37.02	2.02	5.46	25.83	2.75	10.64
SFRC1.00	89.17	6.57	7.36	38.89	0.86	2.20	37.57	0.80	2.13	23.55	0.86	3.64

The estimated fiber content in cubic specimens was slightly higher than the expected value. Based on the mixture compositions, the expected fiber contents were 39.25 kg/m³, 58.88 kg/m³, and 78.5 kg/m³ for SFRC0.50, SFRC0.75, and SFRC1.00, respectively. However, the observed contents were 46.19 kg/m³, 63.76 kg/m³, and 89.17 kg/m³ for SFRC0.50, SFRC0.75, and SFRC1.00, respectively.

The fiber orientation along the x and y axes was consistent across specimens and surpassed the fiber orientation along the z axes, indicating a preferential horizontal plane in the fiber distribution across all compositions. This phenomenon may be attributed to the uniformity of wall effects along both the x and y directions within a cubic specimen. The least contribution of fibers was observed in the z-direction, perpendicular to the horizontal plane, attributed to the influence of gravity and vibration. The fracture plane of the MVD test aligns with the y-z plane of the inductance test.

3.5 Residual tensile strength from MVD test

Figure 13 shows the Load vs. CMOD curves of all the specimens. The curves from the 28-day tests were presented in gray, while those from the 100-day tests were shown in purple. The average curves were emphasized with bold lines. All specimens showed "softening" behavior and, therefore, met the methodology proposed by Segura-Castillo et al. [18]. Similarly to the 3PBT, the load values increased with the addition of fiber content for both ages, demonstrating the contribution of the fibers.

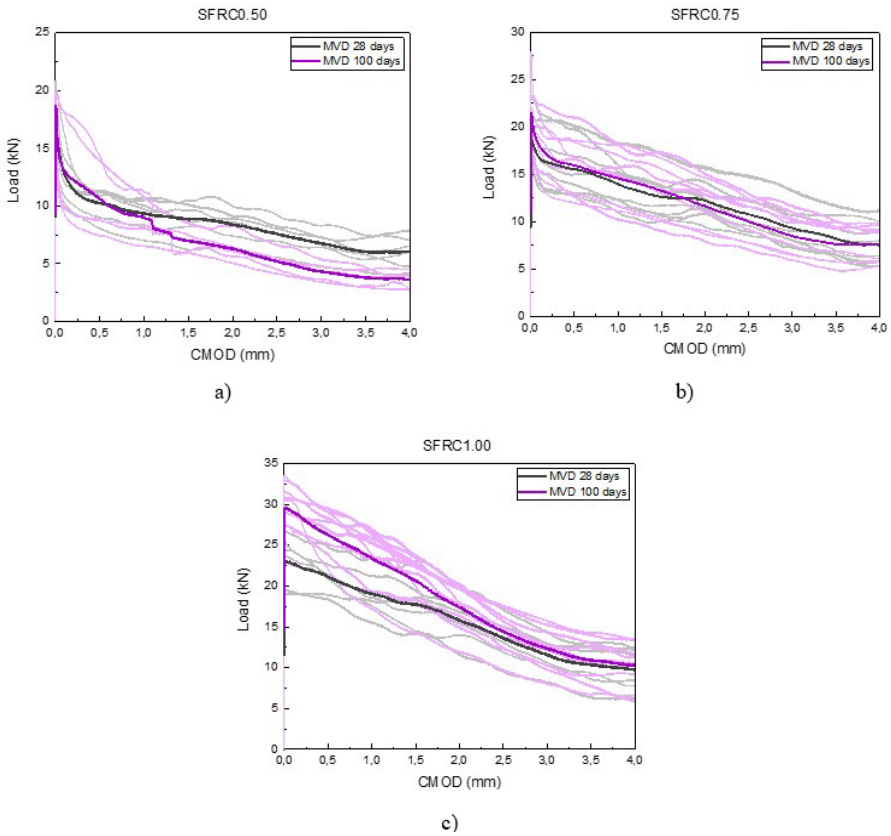

Figure 13. Load vs. CMOD test MVD: a) SFRC0.50; b) SFRC0.75; c) SFRC1.00.

Table 6 shows the results at 28 days and 100 days, showcasing the average peak load (F_{Peak}) and average residual loads (F_{R1}, F_{R2}, F_{R3}, and F_{R4}). Theses values were determined at CMOD levels of 0.5, 1.5, 2.5, and 3.5, respectively, for cubic specimens and half-prismatic specimens. The table includes average values for each variable, as well as standard deviation (SD) and coefficient of variation (CV).

Generally, for the same concrete mix and at both ages, the loads obtained from half-prismatic specimens were lower than those from cubic specimens. This observation underscores the influence of specimen size, shape, and casting process on the distribution of fibers and, consequently, on the residual tensile load determined by the MVD test.

Table 6. Loads from MVD test.

Concrete	Variable	Loads at 28 days (kN)					Loads at 100 days (kN)				
		Cubic	Half-prismatic	Average	SD	CV (%)	Cubic	Half-prismatic	Average	SD	CV (%)
SFRC0.50	F_{Peak}	18.37	17.95	18.16	2.24	12.31	19.86	18.53	19.19	1.01	5.28
	F_{R1}	11.19	9.83	10.51	1.39	13.22	13.94	9.49	11.72	2.89	24.68
	F_{R2}	9.88	8.38	9.13	1.56	17.05	8.47	6.59	7.53	1.06	14.05
	F_{R3}	8.13	7.29	7.71	1.27	16.43	6.59	4.84	5.71	0.95	16.67
	F_{R4}	6.72	5.74	6.23	1.19	19.06	4.65	3.60	4.13	0.78	18.84
SFRC0.75	F_{Peak}	18.96	18.55	18.75	2.38	12.70	19.69	22.95	21.32	3.26	15.27
	F_{R1}	16.47	14.65	15.56	3.00	19.30	16.73	15.51	16.11	3.07	19.03
	F_{R2}	13.86	11.47	12.66	2.36	18.65	13.50	13.11	13.30	3.00	22.54
	F_{R3}	12.02	9.55	10.78	2.13	19.71	10.92	9.69	10.31	2.33	22.61
	F_{R4}	9.63	6.94	8.28	2.13	25.73	8.62	7.44	8.03	2.08	25.86
SFRC1.00	F_{Peak}	22.54	24.75	23.64	3.12	13.20	31.30	28.00	29.65	3.08	10.39
	F_{R1}	21.17	21.16	21.17	2.38	11.27	27.97	24.63	26.30	3.06	11.62
	F_{R2}	18.80	15.64	17.22	3.38	19.63	21.41	20.06	20.74	3.10	14.96
	F_{R3}	14.08	12.46	13.27	2.67	20.10	13.91	14.86	14.39	2.45	17.04
	F_{R4}	11.11	9.00	10.06	2.69	26.74	10.20	11.78	10.99	2.56	23.29

Comparing the peak load results for different ages for the same type of concrete, it was observed that for SFRC0.50 and SFRC0.75, there was no significant difference between the results for 28 and 100 days. However, for SFRC1.00, a notable disparity in the average peak load between tests at 28 and 100 days was identified, suggesting an increase in tensile strength over the analyzed period. The disparity observed in SFRC1.00 likely arose from variations in the number of fibers intersecting the fracture plane.

Concerning residual loads, for SFRC0.50, there was no significant difference in F_{R1} between the results at 28 and 100 days, while a significant difference was observed for F_{R2} to F_{R4}, with higher values at 28 days. In the case of SFRC0.75, there was no significant difference for any of the residual loads (F_{R1} to F_{R4}) between the ages 28 and 100-day results. In contrast, for SFRC1.00, a significant difference was noted in F_{R1} between the results for 28 and 100 days, and no significant difference was observed for F_{R2} to F_{R4} for the analyzed periods.

3.6 Residual tensile strength from three-point bending test vs. MVD test

The mechanical response of the MVD test demonstrated comparable performance to the 3PBT test outlined in NBR 16940 [11] and EN 14651 [12]. Equation (8) defines the load correlation factor (k_{MVD}) that establishes a correlation between the two tests, where F_{EN} represents the load in the 3PBT test, and F_{MVD} represents the load in the MVD test. Figure 14 presents the load correlation factor vs. CMOD from specimens' tests at 28 days.

$$k_{MVD} = \frac{F_{EN}}{F_{MVD}} \tag{8}$$

The load correlation factor exhibited a reduction with an increase in fiber volume. Beyond CMOD equals to 2 mm, the values stabilized at approximately 1.90, 1.8, and 1,5 for SFRC0.050, SFRC0.75, and SFRC1.00, respectively. Segura-Castillo, Monte and Figueiredo [18] observed that, in the post-crack region, the k_{MVD} value increases until reaching a CMOD of 2 mm, where it stabilizes at a correlation factor of 2.5. However, their study tested the same concrete derived from similar specimens, featuring a compressive strength of 35 MPa and 20 kg/m^3 of steel fibers with hooked ends (0.25% of fiber content).

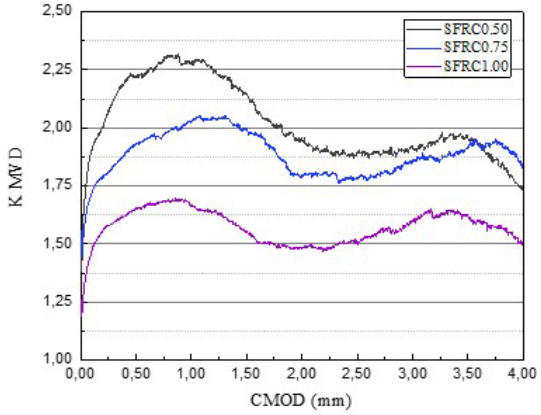

Figure 14. Load correlation factor vs. CMOD at 28 days.

Table 7 shows the k_{MVD} from this study at 28 days, considering only the MVD load results from half-prismatic specimens at CMOD values of 0.5, 1.5, 2.5, and 3.5 mm. Across all compositions, the k_{MVD} values decrease with higher fiber content, and stabilization was observed from the F_{R1} load.

Table 7. k_{MVD} coefficient at 28 days.

Load	SFRC0.50	SFRC0.75	SFRC1.00
F_{Peak}	1.44	1.66	1.43
F_{R1}	2.32	2.05	1.65
F_{R2}	2.27	2.20	1.75
F_{R3}	1.97	2.01	1.63
F_{R4}	2.03	2.27	1.85

Figure 15 illustrates the correlation between the loads obtained 3PBT and the estimated loads from the MVD test, all at 28 days. It is highlighted that this analysis considered only MVD loads from half-prismatic specimens resulting from the NBR 16940/EN 14651 test. Upon comparing the obtained loads, a correlation coefficient of 0.87763 was observed, indicating a reasonable correlation of results.

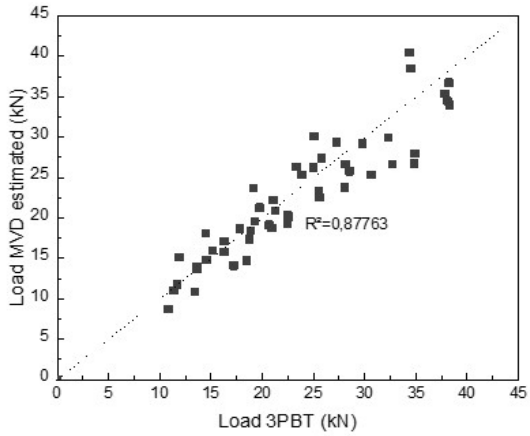

Figure 15. Load comparison 3PBT vs. MVD estimates at 28 days

4 CONCLUSIONS

In this study, the Montevideo (MVD) test was employed as an alternative approach to the three-point bending test to evaluate the tensile behavior and quality control of steel fiber-reinforced concrete. The results lead to the following conclusions:

(1) The addition of fibers did not result in higher compressive strength, as the concrete maintained an approximate strength of 72.5 MPa across the different fiber volumes. On the other hand, the modulus of elasticity exhibited a significant increase, especially with the highest fiber volume.
(2) The fiber orientation in the x and y directions were similar, suggesting the existence of a preferred horizontal plane in the distribution of fibers across all compositions.
(3) In the MVD test, a typical Load vs. CMOD curve also exhibited softening behavior as in the 3PBT test.
(4) A load correlation factor (k_{MVD}) was derived to convert the loads from the MVD test to the NBR 16940 [11] and EN 14651 [12] test at 28 days. The k_{MVD} beyond CMOD 2 mm decreased by 5.6% from SFRC0.50 to SFRC0.75 and by 20% from SFRC0.75 to SFRC1.00 concrete.
(5) MVD test offers a practical and simple method for routine quality control of SFRC. While this quality control method does not replace the necessity of material qualification through the NBR 16940 [11] and EN 14651 [12], it does provide a viable alternative procedure, with a correlation of 0.87763 between the loads estimated from the MVD test and the three-point bending test.

ACKNOWLEDGEMENTS

The authors would like to thank the Graduate Program in Civil Engineering at the Federal University of Paraná (PPGEC/UFPR), the Center for Civil Engineering Studies (CESEC) for the institutional support, the project CNPq/MCTI/FNDCT Nº 18/2021 422189/2021-9, CNPq - grant number: 316985/2021-0, and the institutional project CAPES-PRINT/UFPR for the financial support.

REFERENCES

[1] A. Meda, F. Minelli, and G. A. Plizzari, "Flexural behavior of RC beams in fibre reinforced concrete," *Compos., Part B Eng.*, vol. 43, no. 8, pp. 2930–2937, 2012, http://doi.org/10.1016/j.compositesb.2012.06.003.

[2] F. Abed and M. K. Sabbagh, “Shear response of BFRP-reinforced short beams using fiber reinforced concrete,” in *Proc. 10th Int. Conf. FRP Comp. Civ. Eng.*, 2022, http://doi.org/10.1007/978-3-030-88166-5_27.

[3] J. H. Lee, "Influence of concrete strength combined with fiber content in the residual flexural strengths of fiber reinforced concrete," *Compos. Struct.*, vol. 168, pp. 216–225, 2017, http://doi.org/10.1016/j.compstruct.2017.01.052.

[4] M. Di Prisco, G. Plizzari, and L. Vandewalle, "Fibre reinforced concrete: new design perspectives," *Mater. Struct.*, vol. 42, no. 9, pp. 1261–1281, 2009, http://doi.org/10.1617/s11527-009-9529-4.

[5] X. Liu, Q. Sun, Y. Yuan, and L. Taerwe, "Comparison of the structural behavior of reinforced concrete tunnel segments with steel fiber and synthetic fiber addition," *Tunn. Undergr. Space Technol.*, vol. 103, pp. 103506, 2020, http://doi.org/10.1016/j.tust.2020.103506.

[6] I. L. Larsen and R. T. Thorstensen, "The influence of steel fibres on compressive and tensile strength of ultra high performance concrete: a review," *Constr. Build. Mater.*, vol. 256, pp. 119459, 2020, http://doi.org/10.1016/j.conbuildmat.2020.119459.

[7] B. Li, L. Xu, Y. Shi, Y. Chi, Q. Liu, and C. Li, "Effects of fiber type, volume fraction and aspect ratio on the flexural and acoustic emission behaviors of steel fiber reinforced concrete," *Constr. Build. Mater.*, vol. 181, pp. 474–486, 2018, http://doi.org/10.1016/j.conbuildmat.2018.06.065.

[8] Réunion Internationale des Laboratoires et Experts des Matériaux, *Test and Design Methods for Steel Fibre Reinforced Concrete Sigma-Epsilon-Design Method*, RILEM TC 162-TDF, 2003.

[9] Federation Internationale du Beton, *FIB Model Code for Concrete Structures*, 2010.

[10] National Research Council, *Guide for the Design and Construction of Fiber Reinforced Concrete Structures*, CNR-DT 204, 2006.

[11] Associação Brasileira de Normas Técnicas, *Fiber Reinforced Concrete – Determination of the Flexure Tensile Strengths (Limit of Proportionality and Residual Strengths)*, ABNT NBR 16940, 2021. [in Portuguese].

[12] European Committee for Standardization, *Test Method for Metallic Fibre Concrete – Measuring the Flexural Tensile Strength (Limit of Proportionality (Lop), Residual)*, EN 14651, 2005.

[13] A. Amin, S. J. Foster, and A. Muttoni, "Derivation of the σ - w relationship for SFRC from prism bending tests," *Struct. Concr.*, vol. 16, no. 1, pp. 93–105, 2015, http://doi.org/10.1002/suco.201400018.

[14] Associação Brasileira de Normas Técnicas, *Fiber Reinforced Concrete – Determination of Tensile Strength Using Double Punch Test (Cracking and Residuals Strength) – Test Method*, ABNT NBR 16939, 2021. [in Portuguese].

[15] E. Brühwiler and F. H. Wittmann, "The wedge splitting test, a new method of performing stable fracture mechanics tests," *Eng. Fract. Mech.*, vol. 35, no. 1-3, pp. 117–125, 1990, http://doi.org/10.1016/0013-7944(90)90189-N.

[16] C. Molins, A. Aguado, and S. Saludes, "Double punch test to control the energy dissipation in tension of FRC (Barcelona test)," *Mater. Struct.*, vol. 42, no. 4, pp. 415–425, 2009, http://doi.org/10.1617/s11527-008-9391-9.

[17] M. Di Prisco, L. Ferrara, and M. G. L. Lamperti, "Double edge wedge splitting (DEWS): An indirect tension test to identify post-cracking behavior of fibre reinforced cementitious composites," *Mater. Struct.*, vol. 46, no. 11, pp. 1893–1918, 2013, http://doi.org/10.1617/s11527-013-0028-2.

[18] L. Segura-Castillo, R. Monte, and A. D. de Figueiredo, "Characterisation of the tensile constitutive behavior of fibre-reinforced concrete: a new configuration for the Wedge Splitting Test," *Constr. Build. Mater.*, vol. 192, pp. 731–741, 2018, http://doi.org/10.1016/j.conbuildmat.2018.10.101.

[19] P. Pujadas, A. Blanco, S. H. P. Cavalaro, A. de la Fuente, and A. Aguado, "Multidirectional double punch test to assess the post-cracking behavior and fibre orientation of FRC," *Constr. Build. Mater.*, vol. 58, pp. 214–224, 2014, http://doi.org/10.1016/j.conbuildmat.2014.02.023.

[20] Associação Brasileira de Normas Técnicas, *Self-Consolidating Concrete – Part 1: Classification, Control and Receipt in the Fresh State*, ABNT NBR 15823-1, 2017. [in Portuguese].

[21] Associação Brasileira de Normas Técnicas, *Self-Consolidating Concrete – Part 2: Slump-Flow Test, Flow Time and visual Stability Index – Abrams Cone Method*, ABNT NBR 15823-2, 2017. [in Portuguese].

[22] Associação Brasileira de Normas Técnicas, *Concrete – Compression Test of Cylindrical Specimens*, ABNT NBR 5739, 2018. [in Portuguese].

[23] American Society for Testing and Materials, *Standard Test Method for Compressive Strength of Cylindrical Concrete Specimens*, ASTM C39/C39M-18, 2018, p. 8.

[24] Associação Brasileira de Normas Técnicas, *Hardened Concrete – Determination of Elasticity and Deformation Modulus. Part 1: Static Modulus by Compression*, ABNT NBR 8522-1, 2021. [in Portuguese].

[25] American Society for Testing and Materials, *Standard Test Method for Static Modulus of Elasticity and Poisson's Ratio of Concrete in Compression*, ASTM C469/C469M-14, 2014, p. 5.

[26] Associação Brasileira de Normas Técnicas, *Fiber Reinforced Concrete – Quality Control*, ABNT NBR 16938, 2021. [in Portuguese].

[27] J. M. Torrents, A. Blanco, P. Pujadas, A. Aguado, P. Juan-García, and M. Á. Sánchez-Moragues, "Inductive method for assessing the amount and orientation of steel fibers in concrete," *Mater. Struct.*, vol. 45, no. 10, pp. 1577–1592, 2012, http://doi.org/10.1617/s11527-012-9858-6.

[28] S. H. P. Cavalaro, R. López, J. M. Torrents, and A. Aguado, "Improved assessment of fibre content and orientation with inductive method in SFRC," *Mater. Struct.*, vol. 48, no. 6, pp. 1859–1873, 2015, http://doi.org/10.1617/s11527-014-0279-6.

[29] R.-D. López et al., "Assessment of fibre content and orientation in SFRC with the inductive method. Part 1: theoretical basis of the method and study of the influence of the type of coil and temperature on its accuracy," *Mater. Struct. Constr*, vol. 48, no. 6, pp. 1859–1873, 2015, http://doi.org/10.1617/s11527-014-0279-6.

[30] C. V. Voigt, R. Pieralisi, M. J. J. Bonfim, S. H. P. Cavalaro, and R. A. Medeiros-Junior, "Numerical and experimental surface inductive for steel fibers," *ACI Mater. J.*, vol. 119, no. 2, pp. 269–279, 2022, http://doi.org/10.14359/51734402.

[31] Associação Brasileira de Normas Técnicas, *Fresh Concrete – Slump Test*, ABNT NBR 16889, 2020. [in Portuguese].

[32] Associação Brasileira de Normas Técnicas, *Concrete for Structural Use – Density, Strength and Consistence Classification*, ABNT NBR 8953, 2015. [in Portuguese].

[33] A. Mudadu, G. Tiberti, F. Germano, G. A. Plizzari, and A. Morbi, "The effect of fiber orientation on the post-cracking behavior of steel fiber reinforced concrete under bending and uniaxial tensile tests," *Cement Concr. Compos.*, vol. 93, no. June, pp. 274–288, 2018, http://doi.org/10.1016/j.cemconcomp.2018.07.012.

[34] O. Tsioulou, A. Lampropoulos, and S. Paschalis, "Combined Non-Destructive Testing (NDT) method for the evaluation of the mechanical characteristics of Ultra High Performance Fibre Reinforced Concrete (UHPFRC)," *Constr. Build. Mater.*, vol. 131, pp. 66–77, 2017, http://doi.org/10.1016/j.conbuildmat.2016.11.068.

[35] D.-Y. Yoo, Y.-S. Yoon, and N. Banthia, "Predicting the post-cracking behavior of normal- and high-strength steel-fiber-reinforced concrete beams," *Constr. Build. Mater.*, vol. 93, pp. 477–485, 2015, http://doi.org/10.1016/j.conbuildmat.2015.06.006.

[36] A. Le Hoang and E. Fehling, "Influence of steel fiber content and aspect ratio on the uniaxial tensile and compressive behavior of ultra high performance concrete," *Constr. Build. Mater.*, vol. 153, pp. 790–806, 2017, http://doi.org/10.1016/j.conbuildmat.2017.07.130.

[37] N. Suksawang, S. Wtaife, and A. Alsabbagh, "Evaluation of elastic modulus of fiber-reinforced concrete," *ACI Mater. J.*, vol. 115, no. 2, pp. 239–249, 2018, http://doi.org/10.14359/51701920.

[38] M. Gul, A. Bashir, and J. A. Naqash, "Study of modulus of elasticity of steel fiber reinforced concrete," *Int. J. Eng. Adv. Technol.*, vol. 3, no. 4, pp. 304–309, 2014.

[39] Y. Mohammadi, R. Carkon-Azad, S. P. Singh, and S. K. Kaushik, "Impact resistance of steel fibrous concrete containing fibres of mixed aspect ratio," *Constr. Build. Mater.*, vol. 23, no. 1, pp. 183–189, 2009, http://doi.org/10.1016/j.conbuildmat.2008.01.002.

[40] Z. Wu, C. Shi, W. He, and L. Wu, "Effects of steel fiber content and shape on mechanical properties of ultra high performance concrete," *Constr. Build. Mater.*, vol. 103, pp. 8–14, 2016, http://doi.org/10.1016/j.conbuildmat.2015.11.028.

[41] M. Pourbaba, E. Asefi, H. Sadaghian, and A. Mirmiran, "Effect of age on the compressive strength of ultra-high-performance fiber-reinforced concrete," *Constr. Build. Mater.*, vol. 175, pp. 402–410, 2018, http://doi.org/10.1016/j.conbuildmat.2018.04.203.

[42] R. Wang and X. Gao, "Relationship between flowability, entrapped air content and strength of UHPC mixtures containing different dosage of steel fiber," *Appl. Sci.*, vol. 6, no. 8, pp. 216, 2016, http://doi.org/10.3390/app6080216.

[43] W. Meng and K. H. Khayat, "Effect of hybrid fibers on fresh properties, mechanical properties, and autogenous shrinkage of cost-effective UHPC," *J. Mater. Civ. Eng.*, vol. 30, no. 4, pp. 04018030, 2018, http://doi.org/10.1061/(ASCE)MT.1943-5533.0002212.

[44] L. Liao, J. Zhao, F. Zhang, S. Li, and Z. Wang, "Experimental study on compressive properties of SFRC under high strain rate with different fiber content and aspect ratio," *Constr. Build. Mater.*, vol. 261, pp. 119906, 2020, http://doi.org/10.1016/j.conbuildmat.2020.119906.

[45] L. Rizzuti and F. Bencardino, "Effects of fibre volume fraction on the compressive and flexural experimental behaviour of SFRC," *Contemp. Eng. Sci.*, vol. 7, no. 5–8, pp. 379–390, 2014, http://doi.org/10.12988/ces.2014.4218.

[46] S. Abbas, A. M. Soliman, and M. L. Nehdi, "Exploring mechanical and durability properties of ultra-high performance concrete incorporating various steel fiber lengths and dosages," *Constr. Build. Mater.*, vol. 75, pp. 429–441, 2015, http://doi.org/10.1016/j.conbuildmat.2014.11.017.

[47] T. L. Resende and D. C. T. Cardoso, "Experimental investigation of the shear behavior of steel fiber reinforced concrete slender beams without stirrups through crack kinematics and shear transfer mechanisms," *Struct. Concr.*, vol. 24, no. 4, pp. 4779–4798, 2023, http://doi.org/10.1002/suco.202201057.

Author contributions: GMCB: conceptualization, methodology, formal analysis, data curation, writing; RP: formal analysis, writing, supervision; RDM: formal analysis, writing, supervision.

Editors: José Marcio Calixto, Daniel Carlos Taissum Cardoso.